Procedia Computer Science

Volume 51, 2015, Pages 1897–1906

ICCS 2015 International Conference On Computational Science

Transition Metal Nitride Catalysts for Electrochemical Reduction of Nitrogen to Ammonia at Ambient Conditions

Younes Abghoui and Egill Skúlasson

Science Institute and Faculty of Physical Sciences, VR-III, University of Iceland, IS-107 Reykjavík, Iceland

yoa2@hi.is and egillsk@hi.is

Abstract

Computational screening for catalysts that are stable, active and selective towards electrochemical reduction of nitrogen to ammonia at room temperature and ambient pressure is presented from a range of transition metal nitride surfaces. Density functional theory (DFT) calculations are used to study the thermochemistry of cathode reaction so as to construct the free energy profile and to predict the required onset potential via the Mars-van Krevelen mechanism. Stability of the surface vacancy as well as the poisoning possibility of these catalysts under operating conditions are also investigated towards catalyst engineering for sustainable ammonia formation. The most promising candidates turned out to be the (100) facets of rocksalt structure of VN, CrN, NbN and ZrN that should be able to form ammonia at -0.51 V, -0.76 V, -0.65 V and -0.76 V vs. SHE, respectively. Another interesting result of the current work is that for the introduced nitride candidates, hydrogen evolution is no longer the competing reaction; thus, high formation yield of ammonia is expected at low onset potentials.

Keywords: DFT calculations, Electrochemical synthesis of ammonia, Electrochemical reduction of N_2 to NH_3, Transition metal nitride catalysts

1 Introduction

Ammonia is one of the highly produced chemicals in the globe, which is primarily used in production of fertilizer [1, 2]. Since hundred years ago, ammonia has been synthesized mainly through the Haber-Bosch process where gaseous nitrogen and hydrogen are passed over a Ru- or Fe-based catalyst at high pressure and high temperature to form NH_3 as: [3]

$$N_2(g) + 3H_2(g) \rightarrow 2NH_3(g) \quad (1)$$

Selection and peer-review under responsibility of the Scientific Programme Committee of ICCS 2015

doi:10.1016/j.procs.2015.05.433

The required hydrogen gas for this process is often provided by natural gas, which leads to increased production of various greenhouse gases. The alternative is to produce hydrogen from water splitting, which is a cleaner but very energy intensive process. The Haber-Bosch process is in stark contrast to the function of the enzyme nitrogenase in bacteria in which ammonia is produced from solvated protons, electrons and atmospheric nitrogen at ambient conditions. The active site of the enzyme is a $MoFe_7S_9N$ cluster that catalyzes the electrochemical reaction:

$$N_2 + 8H^+ + 8e^- \rightarrow 2NH_3 + H_2 \quad (2)$$

The source of energy for this reaction is at least 16 adenosine triphosphate (ATP) molecules [4], which are used to increase the chemical potential of the electrons and the protons. Therefore, it is possible that this natural process could be emulated in a man-made and commercial installation. Instead of a separate hydrogen production process, the protons could come from an acidic solution while the electrons would be driven to the electrode surface by an applied electric potential. Various potential routes for ammonia synthesis at ambient conditions are currently being explored (see Refs. 1,2 and 8 for recent reviews). To increase the yields of ammonia, solid-state proton conductors have been employed; resulting in up to 78% conversion of cathodic supplied nitrogen to ammonia [5, 6]. Ionic liquids or molten salts also promote ammonia formation from low current efficiencies up to 72% at high temperatures [7, 8, 9]. While having achieved low-pressure ammonia synthesis, the abovementioned studies still suffer from the requirement of relatively high temperatures, which leads to increased product decomposition. Another drawback is the use of complex and expensive electrolytes that hinder commercialization. To the best of the authors' knowledge, the first observations of ammonia synthesis at milder conditions were reported with homogeneous catalysts with tungsten [10] and zirconium [11] as the central atoms. However, for the sake of distributed use of ammonia, simpler methods are needed, ideally using heterogeneous catalysis, which allows for facile isolation of product.

With advancements in the field of computations and modeling, theoretical investigations have provided deeper insight into catalysis [12, 13, 14, 15, 16, 17, 18, 19, 20, 21, 22, 23, 24, 25, 26]. The use of computations can thus facilitate rational catalyst design, by enabling whole classes of material to be assessed for their suitability as catalysts. The simplest catalyst for electrochemical ammonia formation is a pure transition metal catalyst. In a recent theoretical study, electrochemical formation of ammonia on a range of flat and stepped transition metal surfaces was studied [27]. It was found that many metals require a relatively small overpotential of -0.5 to -1 V vs. SHE to form ammonia in 1 M aqueous electrolyte (pH = 0) at room temperature. However, the hydrogen evolution reaction (HER) can be very fast and severely hinder the production of ammonia unless the surface is covered with N-adatoms, rather than H-adatoms. It was found that the majority of metals are likely covered with H-adatoms at the onset potential of ammonia formation. This is less likely for the early transition metals, however these are known to readily form oxides. Another study used a similar approach on transition metal Nano-clusters [28] to enhance the ammonia activity compared to HER. However, the presence of water in the electrochemical environment will reduce the efficiency of catalyst by blocking its active site due to preferential adsorption of oxygen rather than nitrogen [29].

In the present study, transition metal nitride catalysts are investigated for electrochemical formation of ammonia at ambient conditions. These materials offer the potential advantage of being able to form ammonia by way of a Mars-van Krevelen mechanism [30], in which a surface N atom is reduced to NH_3 and the catalyst later regenerated with gaseous N_2, rather than adsorbing N_2 to the catalyst surface in the first step. Density functional theory (DFT) calculations are used to study the thermodynamics of the cathode reaction. Free energy diagrams are constructed for the electrochemical protonation of surface nitrogen or metal atoms to obtain onset potentials required for the ammonia synthesis on rocksalt and zincblende transition metal mononitride structures. The effect of an external

potential is included using the computational standard hydrogen electrode [12] and the lowest onset potential required to reduce N_2 to ammonia is estimated for each nitride.

2 Methodology

Mononitrides of the naturally occurring d-block metals are considered in the present study, in both the rocksalt (RS) and zincblende (ZB) structures. The low index facets are considered for each crystal structure, the (100) facets of the RS structure and the (110) facets of the ZB structure. Each nitride surface is modeled by 40 atoms in five layers, with each layer consisting of four metal atoms and four nitrogen atoms. The bottom two layers are fixed whereas the top layers as well as the adsorbed species are allowed to relax. Boundary conditions are periodic in the x and y directions and surfaces are separated by 12 Å of vacuum in the z direction. The structural optimization is considered converged when the forces in any direction on all moveable atoms are less than 0.01 eV/Å. A previous study showed several of the 3d mononitrides to be either antiferromagnetic (RS structure of VN, CrN, MnN, FeN and ZB structure of MnN) or ferromagnetic (ZB structure of VN, CrN) at their equilibrium lattice constants and as such are treated as spin-polarized [31]. The RPBE lattice constants are also taken from that study. The calculations are conducted with density functional theory (DFT) using the RPBE exchanges correlation functional [32]. A plane wave basis set with an energy cutoff of 350 eV is used to represent the valence electrons with a PAW [33] representation of the core electrons as implemented in the VASP code [34]. Activation energies are calculated as the highest point along the minimum energy path (MEP) calculated using the climbing image nudged elastic band method (CI-NEB) [35]. The self-consistent electron density is determined by iterative diagonalization of the Kohn-Sham Hamiltonian, with the occupation of the Kohn-Sham states being smeared according to a Fermi-Dirac distribution with a smearing parameter of kBT = 0.1 eV. A 4 × 4 × 1 Monkhorst-Pack k-point sampling is used for all the surfaces.

3 Results and Discussion

3.1 Stability of the surface nitrogen vacancy

In the Mars-van Krevelen mechanism considered in the present work, a surface nitrogen atom is reduced to form NH_3 after which the resulting vacancy is replenished by a gaseous N_2 molecule. For this replenishment to occur, the N-vacancy needs to be stable at the surface. If this is not the case, the N-vacancy may migrate to the bulk of the catalyst, that is, the reacted nitrogen on the surface is replaced with more nitrogen from the catalyst itself, rather than with gaseous N_2. This process can, in principle, continue until all the nitrogen atoms of the metal nitride have reacted and formed NH_3, leaving only the pure metal. The stability of the N-vacancy at the surface of the catalyst is estimated by comparing the difference in energy of a nitride slab with a single N-vacancy in the surface layer (E_{vac},1) and to that of a single N-vacancy in the first subsurface layer (E_{vac},2). The minimum energy configuration of each of these slabs is found and the energy difference (ΔE_{vac} = (E_{vac},2) - (E_{vac},1)) used as an estimation of the thermodynamic stability of the vacancy at the surface of the nitride. Activation barriers for vacancy migration ($E_{a,vac}$) are also calculated and both ΔE_{vac} and $E_{a,vac}$ are presented in Fig. 1. It is found that, for most of the nitrides, it is thermodynamically favorable for the vacancy to migrate to the bulk, with ΔE_{vac} less than or close to zero. However, it is clear that many of the nitrides exhibit a high activation barrier for vacancy migration and are thus likely to demonstrate a stable surface vacancy. All nitrides with an activation barrier for a vacancy migration of > 1 eV is retained

for further screening, since a barrier of such magnitude is unlikely to be overcome at room temperature.

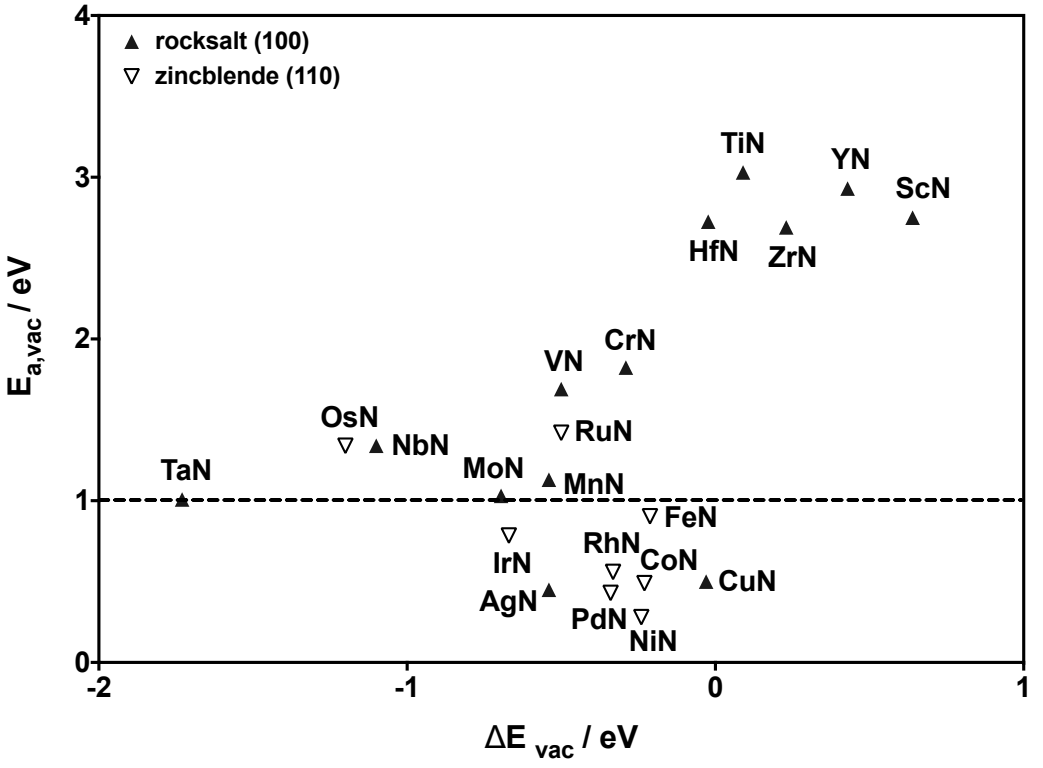

Figure 1: Energy differences (ΔE_{vac}) of a vacancy at the surface layer and in the first subsurface layer of a nitride and the associated activation barrier of vacancy migration ($E_{a,vac}$). The dashed line at $E_{a,vac}$ = 1 eV represents the cutoff above which metal nitrides are considered sufficiently stable for further study.

3.2 Catalytic activity

The rate-determining step (RDS) and our measure of the catalytic activity towards NH_3 formation on each nitride is identified as the elementary reaction step with the largest increase in free energy. When this elementary step can be eliminated by applying a bias, it is referred to as the onset potential, which is the bias that needs to be applied in order to shift the free energy landscape in such a way that all reaction steps become downhill in free energy. The catalytic activity is studied for the nitrides that exhibit stable vacancy on the surface (with $E_{a,vac}$ > 1 eV, Fig.1) where at each H addition step every possible adsorption site is investigated, including other N atoms, metal atoms and bridging sites.

For VN and RuN (shown in Fig. 2) as well as for CrN, each added H adds to the same N atom, forming one NH_3, then the second, with only 6($H^+ + e^-$) required to form 2NH_3. For ZrN, allowing the H to bind to any surface site results in firstly a surface Zr atom being protonated, and then an N atom. The protonation of N is the RDS in NH_3 formation. A similar case is seen for NbN, where two neighboring Nb atoms are protonated before the RDS, which is protonation of the first surface N. For MnN, 3(*NH_2) and 1(*NH) form before the first ammonia is released and 9($H^+ + e^-$) are needed to form 2NH_3. In this case, no metal atoms are protonated. In contrast, for MoN and OsN, H atoms cover all the metal atoms on the surface as well as surface N atoms and 12($H^+ + e^-$) and 13($H^+ + e^-$) are

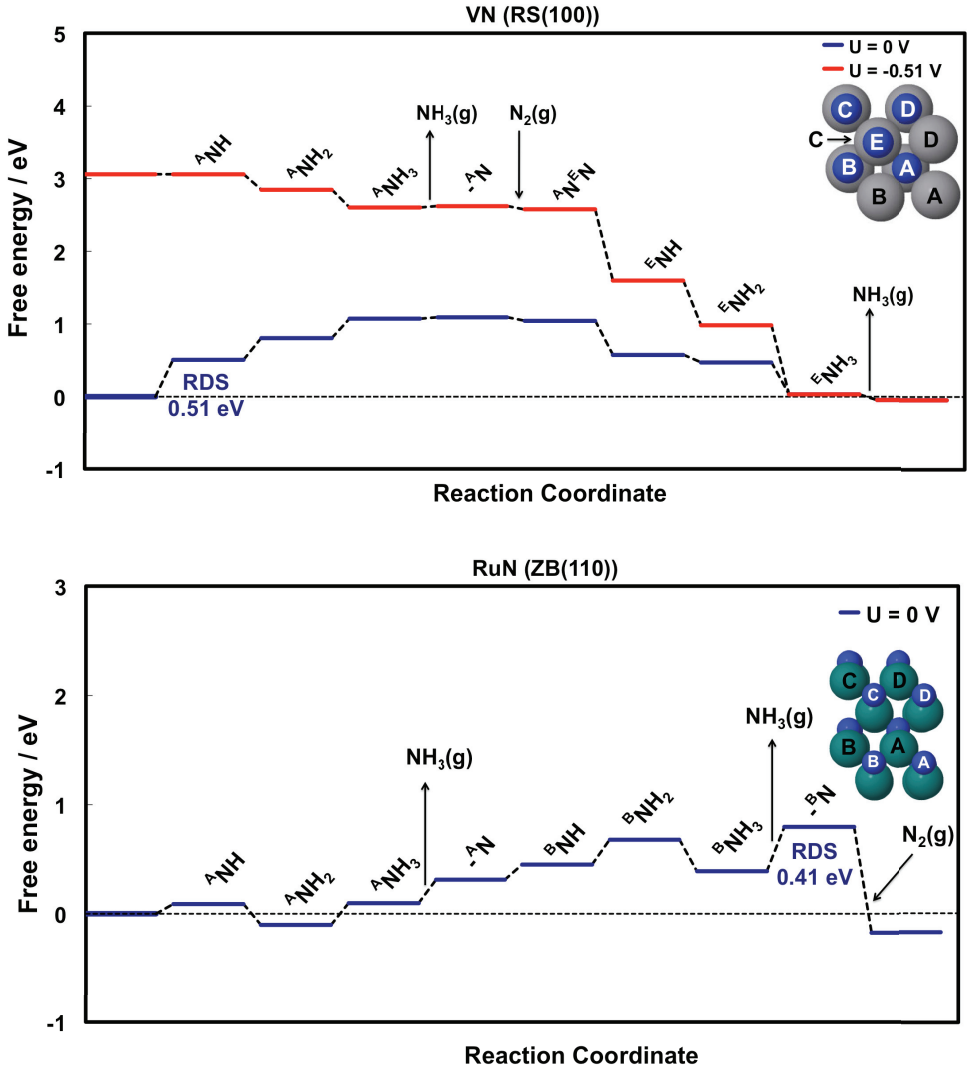

Figure 2: Free energy diagram for NH_3 formation via Mars-van Krevelen mechanism on the (100) facet of RS structure of VN and the (110) facet of ZB structure of RuN. For VN the rate-determining step is the first protonation step with ΔG = 0.51 eV. The blue line indicates the free energy of all the stable intermediates calculated at zero potential. The red line represents the free energy of all the stable intermediates at the onset potential. For RuN the RDS is to release the ammonia with ΔG = 0.41 eV. As the RDS involves no proton-electron transfer, no bias is applied and the free energy landscape of RuN is depicted only at zero potential.

needed to form $2NH_3$. For MoN, to form NH is the RDS. For OsN addition of N_2(g) to fill the N-vacancy is endothermic, which corresponds to an increase in free energy that cannot be surpassed by an external applied bias as no proton-electron transfer is involved at this step. For such cases that require more than the minimum $6(H^+ + e^-)$ to form $2NH_3$, a lower faradaic efficiency is likely to be observed. For TiN, YN, ScN, HfN and TaN an unconstrained mechanism yields a full H coverage on the surface with no NH_3 formation. The catalytic activity of these nitrides are thus instead being considered as potential hydrogen evolution catalysts, the results of which are beyond the scope of the present study. After exclusion of those nitrides that do not form NH_3 (TiN, TaN, ScN, YN and HfN),

eight metal nitride catalysts are considered potentially active towards NH_3 formation and presented in Fig. 3. The RuN from ZB as well as the six RS nitrides shown in Fig.3 should make ammonia electrochemically under ambient conditions whereas ZB OsN likely requires high pressure to fill the N-vacancy in order to complete the catalytic cycle of ammonia formation.

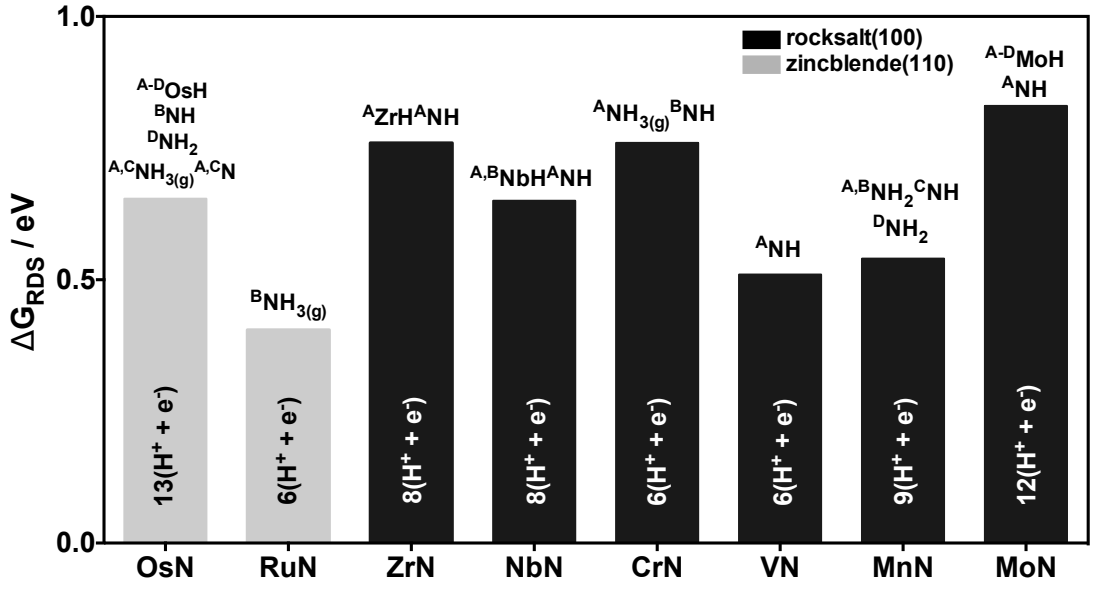

Figure 3: Free energy change (ΔG_{RDS}, in eV) of the rate-determining step of NH_3 formation on transition metal nitride catalysts. At each H addition step every possible adsorption site is investigated including other N atoms, metal atoms and bridging sites and at least $6(H^+ + e^-)$ are needed to form $2NH_3$. The labels above each bar indicate the species formed in the rate-determining step, the notation of which is explained in Fig. 2. The labels in each bar indicate the number of protons and electrons required to make $2NH_3$.

3.3 Poisoning of the surface vacancy

As previously discussed, in the Mars-van Krevelen mechanism considered in this work a surface N is reacted, leaving a surface vacancy at the surface and for the catalytic cycle to complete, this vacancy must be filled with $N_2(g)$. However, there exists the possibility of the vacancy rather being filled with H atoms or O atoms from the aqueous electrolyte, both of which would block this surface site for completion of the catalytic cycle. In the present section the competition between N, O and H for filling the surface vacancy is investigated by considering the free energy of filling the vacancy with O or H relative to N ($\Delta G_{(*N-*X)}$, where X = O or H). These free energies are referenced to N_2, H_2O and H_2 in the gas phase and are calculated at the onset potential for each nitride. A negative value of $\Delta G_{(*N-*X)}$ indicates that it is thermodynamically favorable to fill the vacancy with N, rather than O or H. The values of $\Delta G_{(*N-*X)}$ are shown in Fig. 4 for all the catalytically active nitrides. It can be observed that N atoms bind more strongly to the surface vacancy than O atoms by over 1 eV for most nitrides. Hence, it is not likely for the surface vacancy to be poisoned by O atoms. For poisoning by H, though, the surface vacancy in MnN, MoN and RuN is likely to be filled by H, rather than N. For the remaining nitrides, ZrN, NbN, CrN and VN, the vacancy is likely refilled by N and thus the catalytic cycle may continue to form the second NH_3. These results are as expected as when the bias is tuned

towards more negative values, the electropositive O species bind weaker on the surface compared to H_2O in the gas phase, as they would rather form bonds with the surface when the bias is more positive:

$$H_2O + * \rightarrow *O + 2H^+ + 2e^- \quad (3)$$

Conversely, the H adsorption free energy becomes more negative when the bias is lowered:

$$H^+ + e^- \rightarrow * H \quad (4)$$

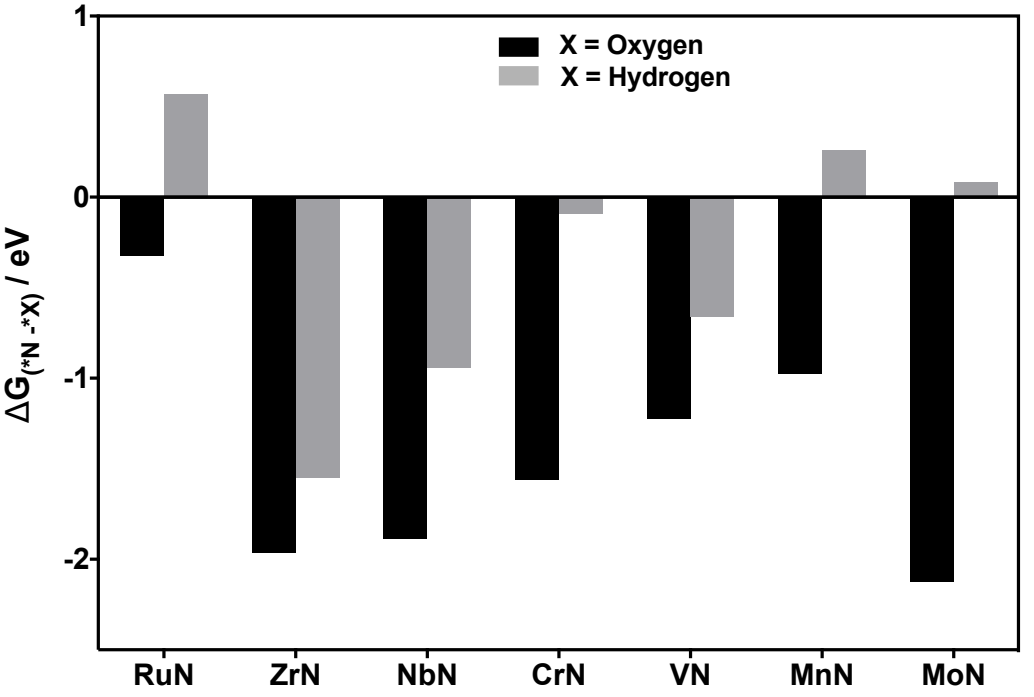

Figure 4: Free energy of adsorption of O or H (relative to N) to the surface vacancy of catalytically active nitrides ($\Delta G_{(*N-*X),}$ in eV). Free energies are calculated relative to N_2(g), H_2(g) and H_2O(g). All free energies are evaluated at the calculated onset potential for each nitrides: ZrN, -0.76 V; NbN, -0.65 V; CrN, -0.76 V; VN, -0.51 V; MnN, -0.54 V; MoN, -0.83 V; and RuN, -0.41 V.

4 Summary and Conclusions

In this paper, first principles calculations are used to screen for nitrogen reduction electrocatalysts that efficiently form ammonia at ambient conditions and in aqueous electrolyte. The most promising nitride catalysts are the (100) facets of rocksalt structure of ZrN, NbN, CrN and VN. The suggested catalysts should have stable N-vacancy at the surface and not be poisoned by oxygen or hydrogen from the aqueous electrolyte. In contrast to previous studies where relatively high onset potentials are required for ammonia formation, and hydrogen evolution is a competing reaction, the most promising RS candidates presented in this paper only need a low applied bias to form ammonia and the competing HER is suppressed. Therefore, a significant amount of ammonia compared with hydrogen gas can be expected. Furthermore, at the onset potential, the N-vacancy is stable towards both

protonation and oxidation from water and it should get easily repaired with atmospheric nitrogen injected to the system at ambient conditions. Other crystal facets and other mechanisms of ammonia formation on these nitride catalysts are currently being studied to further investigate the catalytic capability of this class of catalyst.

5 Acknowledgements

Financial support is acknowledged from the Icelandic Research Fund, Nordic Energy Research by way of the Nordic Initiative for Solar Fuel Development, the Icelandic Student Innovation Fund, and the Research Fund of the University of Iceland. The calculations were in part carried out on the Nordic high performance computer (Gardar).

References

[1] S. Giddey, S. P. S. Badwal, and A. Kulkarni. Review of electrochemical ammonia production technologies and materials. *Int. J. Hydrogen Energy,* **38** (2013) 14576−14594.

[2] I. A. Amar, R. Lan, C. T. G. Petit, and S. Tao. Solid-state electrochemical synthesis of ammonia: a review. *J. Solid State Electrochem.,* **15** (2011) 1845−1860.

[3] V. Smil. Global Population and the Nitrogen Cycle. *Sci. Am.,* **277** (1997) 76−81.

[4] J. M. Berg, J. L. Tymoczko, and L. Stryer. *Biochemistry*, W. H. Freeman, New York (2002) 988−990.

[5] G. Marnellos and M. Stoukides. Ammonia synthesis at atmospheric pressure. *Science,* **282** (1998) 98−100.

[6] G. Marnellos, S. Zisekas, and M. Stoukides. Synthesis of Ammonia at Atmospheric Pressure with the Use of Solid State Proton Conductors. *J. Catal.,* **193** (2000) 80−87.

[7] T. Murakami, T. Nishikiori, T. Nohira, and Y. Ito. Electrolytic synthesis of ammonia in molten salts under atmospheric pressure. *J. Am. Chem. Soc.,* **125** (2003) 334−335.

[8] T. Murakami, T. Nohira, T. Goto, Y. H. Ogata, and Y. Ito. Electrolytic ammonia synthesis from water and nitrogen gas in molten salt under atmospheric pressure. *Electrochim. Acta.,* **50** (2005) 5423−5426.

[9] T. Murakami, T. Nohira, Y. Araki, T. Goto, R. Hagiwara, and Y. H. Ogata. Electrolytic Synthesis of Ammonia from Water and Nitrogen under Atmospheric Pressure Using a Boron-Doped Diamond Electrode as a Nonconsumable Anode. *Electrochem. Solid-State Lett.,* **10** (2007) E4−E6.

[10] J. Catt, A. J. Pearman, and R. L. Richards. The reduction of mono-coordinated molecular nitrogen to ammonia in a protic environment. *Nature,* **253** (1975) 39−40.

[11] J. Pool, E. Lobkovsky, and P. Chirik. Hydrogenation and cleavage of dinitrogen to ammonia with a zirconium complex. *Nature,* **427** (2004) 527−530.

[12] J. K. Nørskov, J. Rossmeisl, A. Logadottir, L. Lindqvist, J. R. Kitchin, T. Bligaard, and H. Jnsson. Origin of the overpotential for oxygen reduction at a fuel-cell cathode. *J. Phys. Chem. B,* **108** (2004) 17886−17892.

[13] J. Greeley and M. Mavrikakis. Alloy catalysts designed from first principles. *Nat. Mater.,* **3** (2004) 810−815.

[14] K. Honkala, A. Hellman, I. N. Remediakis, A. Logadottir, A. Carlsson, S. Dahl, C. H. Christensen, and J. K. Nørskov. Ammonia synthesis from first-principles calculations. *Science,* **307** (2005) 555−558.

[15] J. Hafner and C. Wolverton. Toward Computational Materials Design : The Impact of Density Functional. *MRS Bull,* **31** (2006) 659−668.

[16] F. Abild-Pedersen, J. Greeley, F. Studt, J. Rossmeisl, T. Munter, P. Moses, E. Skúlason, T. Bligaard, and J. Nørskov. Scaling Properties of Adsorption Energies for Hydrogen-Containing Molecules on Transition-Metal Surfaces. *Phys. Rev. Lett.,* **99** (2007) 0161051−0161054.

[17] F. Studt, F. Abild-Pedersen, T. Bligaard, R. Z. Srensen, C. H. Christensen, and J. K. Nørskov. Identification of non-precious metal alloy catalysts for selective hydrogenation of acetylene. *Science,* **30** (2008) 1320−1322.

[18] H. J. Freund and G. Pacchioni. Oxide ultra-thin films on metals: new materials for the design of supported metal catalysts. *Chem. Soc. Rev.,* **37** (2008) 2224−2242.

[19] J. Greeley, I. E. L. Stephens, A. S. Bondarenko, T. P. Johansson, H. A. Hansen, T. F. Jaramillo, J. Rossmeisl, I. Chorkendorff, and J. K. Nørskov. Alloys of platinum and early transition metals as oxygen reduction electrocatalysts. *Nat. Chem.,* **1** (2009) 552−556.

[20] J. K. Nørskov, T. Bligaard, J. Rossmeisl, and C. H. Christensen. Towards the computational design of solid catalysts. *Nat. Chem.,* **1** (2009) 37−46.

[21] J. K. Nørskov, F. Abild-Pedersen, F. Studt, and T. Bligaard. Density functional theory in surface chemistry and catalysis. *Proc. Natl. Acad. Sci. U. S. A.,* **108** (2011) 937−943.

[22] J. G. Howalt, T. Bligaard, J. Rossmeisl, and T. Vegge. DFT based study of transition metal nano-clusters for electrochemical NH3 production. *Phys. Chem. Chem. Phys.,* **15** (2013) 7785−7795.

[23] V. Tripkovic, M. Vanin, M. Karamad, M. E. Bjrketun, K. W. Jacobsen, K. S. Thygesen, and J. Rossmeisl. Electrochemical CO2 and CO Reduction on Metal-Functionalized Porphyrin-like Graphene. *J. Phys. Chem. C,* **117** (2013) 9187−9195.

[24] A. Verdaguer-Casadevall, D. Deiana, M. Karamad, S. Siahrostami, P. Malacrida, T. W. Hansen, J. Rossmeisl, I. Chorkendorff, and I. E. L. Stephens. Trends in the electrochemical synthesis of H2O2: enhancing activity and selectivity by electrocatalytic site engineering. *Nano Lett.,* **14** (2014) 1603−1608.

[25] A. A. Peterson, F. Abild-Pedersen, F. Studt, J. Rossmeisl, and J. K. Nørskov. How copper catalyzes the electroreduction of carbon dioxide into hydrocarbon fuels. *Energy Environ. Sci.,* **3** (2010) 11311−1315.

[26] Y. Abghoui, A. L. Garden, V. F. Hlynsson, S. Björgvinsdóttir, H. Ólafsdóttir, and E. Skúlason. Enabling electrochemical reduction of nitrogen to ammonia at ambient conditions through rational catalyst design. *Phys. Chem. Chem. Phys.,* **17** (2015) 4909-4918.

[27] E. Skúlason, T. Bligaard, S. Gudmundsdóttir, F. Studt, J. Rossmeisl, F. Abild-Pedersen, T. Vegge, H. Jónsson, and J. K. Nørskov. A theoretical evaluation of possible transition metal electro-catalysts for N2 reduction. *Phys. Chem. Chem. Phys.,* **14** (2012) 1235−1245.

[28] J. Howalt, T. Bligaard, J. Rossmeisl and T. Vegge. DFT based study of transition metal nano-clusters for electrochemical NH3 production. *Phys. Chem. Chem. Phys.,* **15** (2013) 7785−7795.

[29] J. Howalt and T. Vegge. The role of oxygen and water on molybdenum nanoclusters for electro catalytic ammonia production. *Beilstein J. Nanotechnol.,* **5** (2014) 111−120.

[30] P. Mars and D. W. Van Krevelen. Special supplement to chemical engineering science. *Eng. Sci.,* **3** (1954) 41−45.

[31] V. F. Hlynsson, E. Skúlason, and A. L. Garden. A systematic, first-principles study of the structural preference and magnetic properties of mononitrides of the d-block metals. *J. Alloys Compd.,* **603** (2014) 172−179.

[32] B. Hammer, L. Hansen, and J. Nørskov. Improved adsorption energetics within density-functional theory using revised Perdew-Burke-Ernzerhof functionals. *Phys. Rev. B,* **59** (1999) 7413−7421.

[33] P. Blchl. Projector augmented-wave method. *Phys. Rev. B,* **50** (1994) 17953−17979.

[34] G. Kresse and J. Hafner. Ab. initio molecular dynamics for liquid metals. *Phys. Rev. B,* **47** (1993) 558−561.

[35] G. Henkelman, B. P. Uberuaga, and H. Jonsson. A climbing image nudged elastic band method for finding saddle points and minimum energy paths. *J. Chem. Phys.,* **113** (2000) 9901−9904.